

**COMPUTATIONAL SCHEME OF AERODYNAMIC-ACOUSTIC-  
STRUCTURE COUPLING FOR ACOUSTIC EFFECTS ON  
AEROELASTIC STRUCTURES**

by

**YU KOK HWA**

**Thesis submitted in fulfillment of the requirements  
for the degree of  
Master of Science**

**JULY 2011**

## ACKNOWLEDGEMENTS

I would like to express my sincere gratitude and appreciation to my supervisor, Dr. A Halim Kadarman for his help, advice, guidance and support throughout my time at Universiti Sains Malaysia. His supervision and encouragement are deeply acknowledged. I also would like to thank Prof. Harijono Djojodihardjo and Dr. Bambang Basuno for their invaluable thoughts and feel grateful for the opportunity to be under their supervision.

I am also thankful to Dr. Farzad Ismail and Dr. Kamarul Ariffin for their valuable comments and the generosity for sharing their ideas. Their suggestions and discussions are priceless. In addition, a special thank you to all the staffs in School of Aerospace Engineering for their help during my master candidature.

A sincere thank you to Phua Yi Jing, Warapong Krengvirat, Tham Wei Ling, Lee See Yau, Sam Sung Ting, Lee Wai Hong, Kee Li Choo, Tay Hong Kang, Chye Yin Hui, Vizzy Nazira, Mohammed Zubair, Arniza Fitri and others who name may not be mentioned. My time at Universiti Sains Malaysia has been greatly enhanced by the friendships we have formed and at the same time, their presences have been always providing me the endless memories and inspirations throughout my study.

I would also like to express my deep gratitude to my family, especially to my father Yu Boon Chong, my mother Chan Good Luan and my siblings who have always supported and encouraged me. Without their support, this thesis would not be possible. Last but not least, thanks to Ng Teng Teng, who has given me unconditional support. Thank you for sharing the good times as well as the hard ones together.

## TABLE OF CONTENTS

<b>ACKNOWLEDGEMENTS</b>	ii
<b>TABLE OF CONTENTS</b>	iii
<b>LIST OF TABLES</b>	vi
<b>LIST OF FIGURES</b>	vii
<b>NOMENCLATURE</b>	xv
<b>ABSTRAK</b>	xviii
<b>ABSTRACT</b>	xx

### **CHAPTER 1 – INTRODUCTION**

1.1	Overview	1
1.2	Problem Statement	3
1.3	Objectives of Research	4
1.4	Scope of Study	5
1.5	Thesis Hypothesis	6
1.6	Thesis Outline	6

### **CHAPTER 2 – LITERATURE REVIEW**

2.1	Unsteady Aerodynamics Prediction	8
2.2	Suppressing Flutter	14
2.3	Acoustic Effects on Structure	18

### **CHAPTER 3 – COMPUTATIONAL METHODOLOGY**

3.1	Analysis of Free Vibration	22
3.1.1	Introduction	22
3.1.2	Governing Equation of Motion	22
3.1.3	Isoparametric Four-Node Quadrilateral Shell Element	23
3.1.4	Element Mass and Stiffness Matrices	26
3.1.5	Isotropic and Orthotropic Materials	27
3.1.6	Assembly of Global Mass and Stiffness Matrices	28
3.1.7	Natural Frequency and Mode Shape	29

3.2	Forced Response Analysis using Computational Aerodynamics	30
3.2.1	Introduction	30
3.2.2	Two-dimensional Panel Method	31
3.2.3	Two-dimensional Unsteady Panel Method	36
3.2.4	Pressure Coefficients in Frequency Domain	44
3.2.5	Three-dimensional Panel Method	45
3.2.6	Three-dimensional Unsteady Panel Method	49
3.2.7	Aeroelastic Analysis with Aerodynamic Forces	52
3.3	Forced Response Analysis using Aerodynamic-Acoustic-Structure Interaction	54
3.3.1	Introduction	54
3.3.2	Helmholtz Integral Equation	54
3.3.3	Boundary Element Method Formulation	55
3.3.4	Aerodynamic-Acoustic-Structure Coupling	59
3.4	Computational Flow Chart	64

## **CHAPTER 4 – RESULTS AND DISCUSSION**

4.1	Introduction	67
4.2	Structural Analysis	67
4.2.1	Wing Structural Model	67
4.2.2	Free Vibration Analysis	71
	4.2.2.1 Rectangular Wing Model	71
	4.2.2.2 AGARD 445.6 Wing Model	74
4.3	Forced Response Analysis using Computational Aerodynamics	77
4.3.1	Wing Aerodynamic Model	77
4.3.2	Two-dimensional Aerodynamic Analysis	78
	4.3.2.1 Two-dimensional Unsteady Panel Method	78
	4.3.2.2 Two-dimensional Aerodynamic Analysis in Frequency Domain	89
	4.3.2.3 Effect of Reduced Frequency Variations on Pressure Distribution	92

4.3.2.4	Effect of Airfoil Profile Variations on Pressure Distribution	95
4.3.2.5	Effect of Mean Angle of Attack Variations on Pressure Distribution	98
4.3.3	Three-dimensional Aerodynamic Analysis	104
4.3.3.1	Three-dimensional Unsteady Panel Method	105
4.3.3.2	Comparison with Two-dimensional Unsteady Panel Method	107
4.3.3.3	Comparison with Doublet Lattice Method	111
4.3.3.4	Comparison with Other Techniques	114
4.3.4	Flutter Analysis	116
4.4	Forced Response Analysis using Aerodynamic-Acoustic-Structure Interaction	120
4.4.1	Acoustic Modeling	120
4.4.2	Flutter Analysis using Aerodynamic and Acoustic Forces	126
4.4.3	Effect of Uniform Radial Velocity Variations on Flutter Analysis	128
<b>CHAPTER 5 – CONCLUSION</b>		
5.1	Summary	132
5.2	Future work	135
<b>REFERENCES</b>		136
<b>APPENDICES</b>		
APPENDIX A: Doublet Lattice Method Formulation		A1
APPENDIX B: Unsteady Aerodynamic Analysis on Wing Models		B1
APPENDIX C: Acoustic Analysis on Wing Models		C1
<b>PAPERS</b>		
D1: Development and implementation of some BEM variants—A critical review		D1
D2: Acoustic effects on binary aeroelasticity model		D2

## LIST OF TABLES

		<b>Page</b>
Table 4.1	Comparison of natural frequencies for rectangular wing model	73
Table 4.2	Comparison of natural frequencies for AGARD 445.6 wing model	76
Table 4.3	Comparison of flutter speed under various analyses	131

## LIST OF FIGURES

		<b>Page</b>
Figure 2.1	Schematic layout of piezoelectric actuator attachment	16
Figure 2.2	Schematic layout of cantilever wing with trailing edge flap	17
Figure 2.3	Loudspeaker mounted A) within the wing and B) in the wall of wind tunnel	19
Figure 3.1	The four-node quadrilateral element: A) physical coordinates, B) isoparametric coordinates	24
Figure 3.2	Discretized airfoil with notation	32
Figure 3.3	Vortex formation during A) pitch down motion and B) pitch up motion	36
Figure 3.4	Discretization of unsteady panel method with notation for time-steps, A) $t = 0$ , B) $t = 1$ and C) $t = k$	37
Figure 3.5	Representation of core vortex and the corresponding notations with respect to $i$ -th control point	40
Figure 3.6	Discretization of the wing surface using quadrilateral element	45
Figure 3.7	Quadrilateral constant-strength for A) source element, and B) doublet element	46
Figure 3.8	Schematic representation for three-dimensional wing model with wake panels in time-steps	49
Figure 3.9	Schematic FE-BE problem representing quarter space problem domains	59
Figure 3.10	Isometric view of a 3D representation of aeroelastic structure and its surrounding boundary	60
Figure 3.11	Bottom view of aeroelastic structure and its surrounding boundary	60
Figure 3.12	Flow chart for computational scheme (Part 1)	65
Figure 3.13	Flow chart for computational scheme (Part 2)	66

Figure 4.1	Discretization of half span rectangular wing model with dimensions	68
Figure 4.2	Discretization of half span AGARD 445.6 wing model with dimensions	68
Figure 4.3	The finite element model of rectangular wing with numbering of node	69
Figure 4.4	The finite element model of AGARD 445.6 wing with numbering of node	69
Figure 4.5	The first four mode shapes of the rectangular wing model using MSC/NASTRAN and MATLAB	72
Figure 4.6	The first four mode shapes of the AGARD 445.6 wing model using MSC/NASTRAN and MATLAB	75
Figure 4.7	Airfoil profile for NACA 0012	77
Figure 4.8	Airfoil profile for NACA 65A004	77
Figure 4.9	Pressure distribution for airfoil NACA 0012 in steady flow at 0 degree angle of attack	78
Figure 4.10	Pressure distribution for airfoil NACA 65A004 in steady flow at 0 degree angle of attack	79
Figure 4.11	Comparison of pressure distribution for airfoil NACA 0012 between panel method, FLUENT and experimental data	80
Figure 4.12	Comparison of pressure distribution for airfoil NACA 65A004 between panel method and numerical data	80
Figure 4.13	A) Pressure distribution and, B) Pressure difference distribution over airfoil NACA 0012 at 0 degree angle of attack with $t = 0s$	82
Figure 4.14	A) Pressure distribution and, B) Pressure difference distribution over airfoil NACA 0012 at 5 degree angle of attack with $t = 7.854s$	82
Figure 4.15	A) Pressure distribution and, B) Pressure difference distribution over airfoil NACA 0012 at 10 degree angle of attack with $t = 15.708s$	82



Figure 4.16	A) Pressure distribution and, B) Pressure difference distribution over airfoil NACA 0012 at 5 degree angle of attack with $t = 23.562s$	83
Figure 4.17	A) Pressure distribution and, B) Pressure difference distribution over airfoil NACA 0012 at 0 degree angle of attack with $t = 31.416s$	83
Figure 4.18	A) Pressure distribution and, B) Pressure difference distribution over airfoil NACA 0012 at -5 degree angle of attack with $t = 39.27s$	83
Figure 4.19	A) Pressure distribution and, B) Pressure difference distribution over airfoil NACA 0012 at -10 degree angle of attack with $t = 47.124s$	84
Figure 4.20	A) Pressure distribution and, B) Pressure difference distribution over airfoil NACA 0012 at -5 degree angle of attack with $t = 54.978s$	84
Figure 4.21	A) Pressure distribution and, B) Pressure difference distribution over airfoil NACA 0012 at 0 degree angle of attack with $t = 62.832s$	84
Figure 4.22	A) Pressure distribution and, B) Pressure difference distribution over airfoil NACA 65A004 at 0 degree angle of attack with $t = 0s$	85
Figure 4.23	A) Pressure distribution and, B) Pressure difference distribution over airfoil NACA 65A004 at 5 degree angle of attack with $t = 7.854s$	85
Figure 4.24	A) Pressure distribution and, B) Pressure difference distribution over airfoil NACA 65A004 at 10 degree angle of attack with $t = 15.708s$	85
Figure 4.25	A) Pressure distribution and, B) Pressure difference distribution over airfoil NACA 65A004 at 5 degree angle of attack with $t = 23.562s$	86
Figure 4.26	A) Pressure distribution and, B) Pressure difference distribution over airfoil NACA 65A004 at 0 degree angle of attack with $t = 31.416s$	86

Figure 4.27	A) Pressure distribution and, B) Pressure difference distribution over airfoil NACA 65A004 at -5 degree angle of attack with $t = 39.27s$	86
Figure 4.28	A) Pressure distribution and, B) Pressure difference distribution over airfoil NACA 65A004 at -10 degree angle of attack with $t = 47.124s$	87
Figure 4.29	A) Pressure distribution and, B) Pressure difference distribution over airfoil NACA 65A004 at -5 degree angle of attack with $t = 54.978s$	87
Figure 4.30	A) Pressure distribution and, B) Pressure difference distribution over airfoil NACA 65A004 at 0 degree angle of attack with $t = 62.832s$	87
Figure 4.31	Pressure distribution in A) real part and, B) imaginary part over surfaces of airfoil NACA 0012 with $k_\alpha = 0.1$	89
Figure 4.32	Pressure distribution in A) real part and, B) imaginary part over surfaces of airfoil NACA 65A004 with $k_\alpha = 0.1$	89
Figure 4.33	Comparison of pressure distribution in real component for airfoil NACA 0012 between panel method and numerical data	91
Figure 4.34	Comparison of pressure distribution in imaginary component for airfoil NACA 0012 between panel method and numerical data	91
Figure 4.35	Effect of reduced frequency on real component of pressure distribution over upper surface of airfoil NACA 0012	93
Figure 4.36	Effect of reduced frequency on imaginary component of pressure distribution over upper surface of airfoil NACA 0012	93
Figure 4.37	Effect of reduced frequency on real component of pressure distribution over upper surface of airfoil NACA 65A004	94
Figure 4.38	Effect of reduced frequency on imaginary component of pressure distribution over upper surface of airfoil NACA 65A004	94
Figure 4.39	Effect of airfoil profile on real component of pressure distribution over upper surface of airfoils	96

Figure 4.40	Effect of airfoil profile on imaginary component of pressure distribution over upper surface of airfoils	96
Figure 4.41	Effect of airfoil profile on real component of pressure distribution over lower surface of airfoils	97
Figure 4.42	Effect of airfoil profile on imaginary component of pressure distribution over lower surface of airfoils	97
Figure 4.43	Effect of angle of attack on real component of pressure distribution over upper surface of airfoil NACA 0012	99
Figure 4.44:	Effect of angle of attack on imaginary component of pressure distribution over upper surface of airfoil NACA 0012	99
Figure 4.45	Effect of angle of attack on real component of pressure distribution over lower surface of airfoil NACA 0012	100
Figure 4.46	Effect of angle of attack on imaginary component of pressure distribution over lower surface of airfoil NACA 0012	100
Figure 4.47	Effect of angle of attack on real component of pressure distribution over upper surface of airfoil NACA 65A004	101
Figure 4.48	Effect of angle of attack on imaginary component of pressure distribution over upper surface of airfoil NACA 65A004	101
Figure 4.49	Effect of angle of attack on real component of pressure distribution over lower surface of airfoil NACA 65A004	102
Figure 4.50	Effect of angle of attack on imaginary component of pressure distribution over lower surface of airfoil NACA 65A004	102
Figure 4.51	Aerodynamic modeling of AGARD 445.6 wing model with wake panels	102
Figure 4.52	Pressure distribution over rectangular wing on A) upper surface and B) lower surface at 0 degree angle of attack with $t = 0s$	105
Figure 4.53	Pressure distribution over rectangular wing on A) upper surface and B) lower surface at 5 degree angle of attack with $t = 7.854s$	105
Figure 4.54	Pressure distribution over rectangular wing on A) upper surface and B) lower surface at 10 degree angle of attack with $t = 15.708s$	105

Figure 4.55	Pressure distribution over AGARD 445.6 wing on A) upper surface and B) lower surface at 0 degree angle of attack with $t = 0s$	106
Figure 4.56	Pressure distribution over AGARD 445.6 wing on A) upper surface and B) lower surface at 5 degree angle of attack with $t = 7.854s$	106
Figure 4.57	Pressure distribution over AGARD 445.6 wing on A) upper surface and B) lower surface at 10 degree angle of attack with $t = 15.708s$	106
Figure 4.58	Comparison between three-dimensional and two-dimensional panel method on rectangular wing at 0 degree angle of attack with $t = 0s$	108
Figure 4.59	Comparison between three-dimensional and two-dimensional panel method on rectangular wing at 5 degree angle of attack with $t = 7.854s$	108
Figure 4.60	Comparison between three-dimensional and two-dimensional panel method on rectangular wing at 10 degree angle of attack with $t = 15.708s$	109
Figure 4.61	Comparison between three-dimensional and two-dimensional panel method on AGARD 445.6 wing at 0 degree angle of attack with $t = 0s$	109
Figure 4.62	Comparison between three-dimensional and two-dimensional panel method on AGARD 445.6 wing at 5 degree angle of attack with $t = 7.854s$	110
Figure 4.63	Comparison between three-dimensional and two-dimensional panel method on AGARD 445.6 wing at 10 degree angle of attack with $t = 15.708s$	110
Figure 4.64	Pressure distribution in real component over rectangular wing along spanwise direction using DLM and panel method	112
Figure 4.65	Pressure distribution in imaginary component over rectangular wing along spanwise direction using DLM and panel method	112
Figure 4.66	Pressure distribution in real component over AGARD 445.6 wing along spanwise direction using DLM and panel method	113

Figure 4.67	Pressure distribution in imaginary component over AGARD 445.6 wing along spanwise direction using DLM and panel method	113
Figure 4.68	Comparison between three-dimensional unsteady panel method with other techniques in term of real component of pressure difference distribution	115
Figure 4.69	Comparison between three-dimensional unsteady panel method with other techniques in term of imaginary component of pressure difference distribution	115
Figure 4.70-	V-g graph for rectangular wing	117
Figure 4.71	V-f graph for rectangular wing	117
Figure 4.72	V-g graph for AGARD 445.6 wing	118
Figure 4.73	V-f graph for AGARD 445.6 wing	118
Figure 4.74	A) Incident acoustic and B) total acoustic pressure distribution for acoustic source at the center of mid span on rectangular wing. ( $U_a = 1 \times 10^4 \text{ m/s}$ )	121
Figure 4.75	A) Incident acoustic and B) total acoustic pressure distribution for acoustic source at the center of mid span on rectangular wing. ( $U_a = 1 \times 10^5 \text{ m/s}$ )	121
Figure 4.76	A) Incident acoustic and B) total acoustic pressure distribution for acoustic source at the center of mid span on rectangular wing. ( $U_a = 1 \times 10^6 \text{ m/s}$ )	121
Figure 4.77	A) Incident acoustic and B) total acoustic pressure distribution for acoustic source at the center of mid span on AGARD 445.6 wing. ( $U_a = 1 \times 10^4 \text{ m/s}$ )	122
Figure 4.78	A) Incident acoustic and B) total acoustic pressure distribution for acoustic source at the center of mid span on AGARD 445.6 wing. ( $U_a = 1 \times 10^5 \text{ m/s}$ )	122
Figure 4.79	A) Incident acoustic and B) total acoustic pressure distribution for acoustic source at the center of mid span on AGARD 445.6 wing. ( $U_a = 1 \times 10^6 \text{ m/s}$ )	122

Figure 4.80	A) Incident acoustic and B) total acoustic pressure distribution for acoustic source at the height 0.1m on rectangular wing	124
Figure 4.81	A) Incident acoustic and B) total acoustic pressure distribution for acoustic source at the height 0.5m on rectangular wing	124
Figure 4.82	A) Incident acoustic and B) total acoustic pressure distribution for acoustic source at the height 1.0m on rectangular wing	124
Figure 4.83	A) Incident acoustic and B) total acoustic pressure distribution for acoustic source at the height 0.1m on AGARD 445.6 wing	125
Figure 4.84	A) Incident acoustic and B) total acoustic pressure distribution for acoustic source at the height 0.5m on AGARD 445.6 wing	125
Figure 4.85	A) Incident acoustic and B) total acoustic pressure distribution for acoustic source at the height 1.0m on AGARD 445.6 wing	125
Figure 4.86	V-g graph for rectangular wing with and without acoustic influence	126
Figure 4.87	V-f graph for rectangular wing with and without acoustic influence	127
Figure 4.88	V-g graph for AGARD 445.6 wing with and without acoustic influence	127
Figure 4.89	V-f graph for AGARD 445.6 wing with and without acoustic influence	128
Figure 4.90	Effect of uniform radial velocity on V-g graph for rectangular wing	129
Figure 4.91	Effect of uniform radial velocity on V-f graph for rectangular wing	129
Figure 4.92	Effect of uniform radial velocity on V-g graph for AGARD 445.6 wing	130
Figure 4.93	Effect of uniform radial velocity on V-f graph for AGARD 445.6 wing	130

## NOMENCLATURE

Symbols	Meaning
$\alpha$	Angle of attack
$\beta$	Angle
$\delta$	Kronecker's delta
$\phi$	Mode shape
$\phi_{ae}$	Velocity potential
$\lambda$	Eigenvalue
$\mu$	Doublet strength
$\nu$	Poisson's ratio
$\theta$	Inclination angle of panel
$\rho$	Density
$\sigma$	Source strength
$\tau$	Vortex strength
$\omega$	Natural frequency in radian/sec
$\omega_\alpha$	Pitching angular frequency
$\ell$	Perimeter of the airfoil
$\xi, \eta$	Components of isoparametric coordinate
$\Delta_k$	Length of shed vorticity panel
$\Delta C_p$	Pressure coefficient difference
$\Delta S_k$	Area of quadrilateral element
$\Phi$	Modal matrix
$\Phi_s$	Potential with constant source strength
$\Phi_d$	Potential with constant double strength
$\Gamma$	Circulation
$\Theta_k$	Inclination angle of shed vorticity panel
$\Omega$	Fluid domain
$a$	Radius of pulsating sphere
$c$	Speed of sound

$f$	Natural frequency in Hz
$g$	Green's function
$g_s$	Structural damping
$h$	Thickness
$k_\alpha$	Reduced pitching frequency
$k_{ac}$	Acoustic wave number
$r$	Distance
$t$	Time
$q_l, q_m, q_n$	Perturbation velocity components
$x, y, z$	Components of physical coordinate
$\bar{x}, \bar{y}$	Coordinate of control point
$u, v$	Components of local flow velocity
$C_p$	Pressure coefficient
$E$	Young's modulus
$G$	Shear modulus of elasticity
$L$	Chord length
$L_p$	Sound level
$N$	Shape function
$NG$	Number of Gauss points
$R$	Location in the fluid domain
$S$	Boundary of fluid domain
$U_a$	Uniform radial velocity
$V$	Velocity
$W$	Gauss weight factor
$Z_0$	Acoustic characteristic impedance
$\{u\}$	Physical displacement vector
$\{q\}$	Generalized displacement vector
$\{F\}$	External forces vector
<b>B</b>	Strain displacement matrix



<b>C</b>	Physical damping matrix
$\bar{C}$	Generalized damping matrix
<b>D</b>	Elasticity matrix
<b>J</b>	Jacobian matrix
<b>K</b>	Physical stiffness matrix
$\bar{K}$	Generalized stiffness matrix
<b>L</b>	Global coupling matrix between fluid pressure of a BE node with the point forces of the FE node
<b>M</b>	Physical mass matrix
$\bar{M}$	Generalized mass matrix
<b>N</b>	Shape function matrix
<b>T</b>	Global coupling matrix that connects the normal velocity of a BE node with the translational displacements of the FE nodes
<b>A , B , C</b>	Aerodynamic influence coefficient matrices
<b>H , G</b>	Acoustic influence coefficient matrices

### Superscripts

<i>e</i>	Element
<i>n</i>	Component in normal direction
<i>t</i>	Component in tangential direction
<i>G</i>	Global
<i>T</i>	Transpose

### Acronyms

DPM	Doublet Point Method
VLM	Vortex Lattice Method
KFM	Kernel Function Method
DLM	Doublet Lattice Method
BEM	Boundary Element Method
FEM	Finite Element Method
AIC	aerodynamic influence coefficient

# **SKEMA PENGKOMPUTERAN BAGI GANDINGAN AERODINAMIK- AKUSTIK-STRUKTUR DIGUNAKAN BAGI MENGAJI KESAN AKUSTIK TERHADAP STRUKTUR AEROELASTIK**

## **ABSTRAK**

Tesis ini menyajikan pembangunan suatu skema pengkomputeran yang melibatkan gandingan aerodinamik-akustik-struktur dalam mempelajari kesan akustik pada struktur aeroelastik. Untuk masalah sedemikian, ia melibatkan interaksi pelbagai bidang di antara aerodinamik, akustik dan struktur dinamik dalam menyelesaikan masalah acousto-aeroelastik. Peringkat pertama melibatkan pemodelan struktur sayap dengan menggunakan Kaedah Unsur Terhingga (FEM) dan diuji untuk analisis getaran bebas. Pada bahagian aerodinamik, pertimbangan ketat telah dikhususkan kepada asas aerodinamik dalam membina model aerodinamik dengan menggunakan kaedah panel tidak tetap dalam dua and tiga dimesi. Untuk pengesahan, kaedah tersebut dibandingkan dengan perisian komersial seperti FLUENT dan penyelidik lain yang menggunakan teknik utama seperti Doublet Lattice Method (DLM) yang diperoleh dari Blair (1992). Menggunakan taburan tekanan yang dihasilkan oleh kaedah panel tidak tetap, pekali tekanan tidak tetap kemudian ditukarkan dalam bentuk frekuensi sebelum dikumpulkan dalam persamaan aeroelastik. Penyelesaian untuk masalah aeroelastik akhirnya diperoleh dengan kaedah k. Pada bahagian akhir, permodelan akustik dilakukan dengan menggunakan kaedah unsur batas (BEM). Memanfaatkan kaedah BEM, tekanan akustik diperolehi pada permukaan struktur. Selanjutnya, dengan menggabungkan beban aerodinamik dan akustik, persamaan acousto-aeroelastik yang dibangunkan telah terbentuk dan hasilnya ditunjukkan pada struktur sayap. Dua model sayap yang

digunakan dalam kajian ini ialah segi empat tepat dan AGARD 445.6 sayap model. Menggunakan kaedah pengiraan yang dijelaskan, perisian MATLAB telah digunakan untuk membangunkan model dan menganalisis masalah untuk keseluruhan kajian ini. Oleh yang demikian, kajian ini berpusat pada hasil perhitungan dan tidak melibatkan sebarang keputusan eksperimen.

# **COMPUTATIONAL SCHEME OF AERODYNAMIC-ACOUSTIC-STRUCTURE COUPLING FOR ACOUSTIC EFFECTS ON AEROELASTIC STRUCTURES**

## **ABSTRACT**

This thesis presents a development of a computational scheme involving aerodynamic-acoustic-structure coupling in studying the acoustic effects on aeroelastic structure. For this particular problem, it involved multi-disciplinary interaction between aerodynamics, acoustics and structural dynamics in solving the acousto-aeroelastic problem. The first step is to model the wing structural using Finite Element Method (FEM) and tested for the free vibration analysis. In the aerodynamic part, a comprehensive consideration is devoted on aerodynamic basis in developing the aerodynamic model for unsteady subsonic flow using two- and three-dimensional unsteady panel method. For validation, the present method is compared with commercial software like FLUENT and other researchers' work using predominant techniques such as the Doublet Lattice Method (DLM) formulation obtained from Blair (1992). Using the pressure distribution generated by unsteady panel method, the unsteady pressure coefficient is then converted into frequency domain before assembled in the aeroelastic equation. The solution for aeroelastic problem is eventually obtained using k-method. In the last part, the acoustic modeling is carried out using Boundary Element Method (BEM). Utilizing the BEM formulation, the acoustic pressures are obtained on the structure surface. Subsequently, combining the aerodynamic and acoustic loadings, the developed acousto-aeroelastic equation is formed and the outcomes are demonstrated on typical wing structures. Two standard wing models were used in this study and they are rectangular and AGARD 445.6 wing models. Using the described computational approach, MATLAB software is

utilized in order to model and analyze the problem for this entire research. Thus, this study is centered on computational results and no experimental outcomes will be involved.

## **Chapter 1**

### **INTRODUCTION**

#### **1.1 Overview**

In aeronautical field, the stability of an airplane is one serious concern for aeronautics researchers. For decades, the presence of airplane instabilities creates insecurity in each air passenger and one of these instabilities is referred as aeroelasticity problems. Aeroelasticity, defined as the interaction of aerodynamic, elastic, and inertia forces on elastic structure became a major discussion among scholars when such an interaction could potentially become a serious threat after the world witnessed the unexpected collapse of Tacoma Narrows Bridge. Since the discovery of aeroelastic phenomena, extensive efforts have been made by researchers in understanding this interdisciplinary nature. At early development of aeroelasticity studies, researchers have great interest on structural response for slender body when encountering fluid flow especially fast moving air flow which often behaves in unsteady condition. With the existing knowledge obtained from structure dynamics and aerodynamics, they help drove the aeroelasticity technology for the past few decades in which most of these fundamentals were well understood and described in detail as been documented in classic textbook (Bisplinghoff, et al., 1955). These basic principles which were supported by experimental results are proven to be useful for aircraft design engineers to avoid harmful aeroelastic phenomena.

For an aircraft, slender bodies such as aircraft wings, tails, and control surfaces are typically vulnerable to this deadly threat and each of the aeroelastic influence factors need to be taken into consideration upon the design of an aircraft. During the aircraft

design process, the airframe structure optimizations using results from stability tests were performed by designers as early prevention. However, the rapid development of aircraft design makes the future needs for aeroelasticity instabilities prevention hard to foresee. Hence, most of the on-going researches in this particular field are centered in taming this critical threat. One must bear in mind that the aeroelasticity problems would not exist if the structure were perfectly rigid. To do this, one must design heavier structures to make them stiffer in order to allow the structures to withstand the immense air pressure without any significant structural deformations and this could only lead to low performance airplanes. Therefore, much of the attention is then diverted to develop control mechanisms for suppressing the aeroelastic instabilities and this remains a major challenge as recent airplane designs employ composite materials more frequently than before, resulting more likely for aeroelastic problems to occur as they are much lighter. Note that although aeroelasticity is frequently applied on aeronautical applications, this advanced technology is not exclusive only for aerospace problems. A growing demand for aeroelasticity technology can be seen implemented on other related problems such as air flows around bridges, tall building and wind turbines. This shows that the fast growing knowledge is quickly emerging into one of the leading technology that possess a wide potential in interdisciplinary researches and these aeroelasticity related technologies are not capable to be further developed if the risks from aeroelastic problems couldn't be alleviated. For that reason, the aeroelasticity suppression is a topic of major interest and therefore, in this thesis, a new suppression technique is being investigated which examine the possibility of using external acoustic excitation to suppress the aeroelasticity problems.

## 1.2 Problem Statement

The idea of using external acoustic pressure for suppressing the instabilities of aeroelastic model isn't a new initiative. However, past efforts are rather less convincing and more research efforts need to be made using advanced acoustic and aerodynamic modeling to scrutinize the acoustic effects on flexible structure. One of the main concerns for current aeroelastic analysis is centered on reliability of aerodynamic prediction. For example, one of the significant drawbacks is that the previous methods do not take into account the effect of structure thickness or more specifically, the airfoil shape for a wing model. Most of the previous approaches considered the aeroelastic model as zero-thickness and the thickness of the lifting surface cannot be neglected anymore when taking the accuracy of aerodynamic modeling into consideration. The incapability of these methods has been frequently addressed in several research works (Kuo and Morino, 1975; Försching, 1978; Eller and Carlsson, 2003) and thus a new unsteady aerodynamic modeling is needed for advanced aeroelastic analysis. On the other hand, the acoustic modeling poses its own challenge. However, acoustic modeling using existing numerical approach should be sufficient to predict an accurate acoustic pressure distribution on the surface of structure. Later, the most critical part of this research work is to set up the coupling procedure using the estimated pressures generated from air flow and acoustic source. Aside from the computational outcomes, the efficiency and reliability of the proposed computational method will be discussed as part of the key issues addressed in this study.



### 1.3 Objectives of Research

In search for an alternative suppression method for aeroelastic problem, this thesis tries to investigate the possibility of using the external acoustic influence in reducing the chances of flutter on aeroelastic structure. For this purpose, the main concentration is centered on construction of a computational scheme in solving the acoustic-fluid-structure problem by using the combination of Boundary Element Method (BEM), Finite Element Method (FEM) and panel method. In addition, special attention will be given to increase the accuracy of aerodynamic modeling using three-dimensional unsteady panel method. This could lead to an advanced integrated formulation when combining the unsteady aerodynamic forces and the acoustic influences into the aeroelastic equation. Using the developed computational scheme, it can then be implemented on aeroelastic models (i.e. rectangular and AGARD 445.6 wings) to evaluate the aerodynamic performance before proceed to other subsequent objectives.

In response to the key issues mentioned, objectives of this thesis are specified as following:

- To develop a computational scheme of aerodynamic-acoustic-structure coupling.
- To investigate the influence of reduced frequency and airfoil thickness toward the computational of unsteady pressure distribution.
- To explore the effect of distance and strength of the acoustic source on aeroelastic structures.
- To compare the acoustics influence in flutter analysis for two different wing models – rectangular wing and AGARD 445.6 wing.

## 1.4 Scope of Study

In line with the addressed requirements arising from the problem statement, the present work considered computational approach that been deeply inspired by previous studies with an improved aerodynamics modeling. In this thesis, numerical formulation for incompressible subsonic flow is preferred. However, the computational scheme must include the unsteady condition to evaluate the unsteady pressure distribution. To do so, the wake effect has to be taken into consideration. For convenience, the aerodynamic analysis will be carried out for two-dimensional and three-dimensional flows. Then, in order to integrate the aerodynamic forces for aeroelastic purpose, the numerical method will be further extended for dynamic problem involving time and frequency domains. However, not everything is included and it would be next to impossible to take account all the aerodynamic aspects in the study. Those excluded in this study are the influence of viscosity and compressibility. Meanwhile, to simulate the acoustic source, the boundary integral formulation will be used for this study as it is widely demonstrated for acoustic modeling and would allows the simulation of field in unbounded domains. In fact, the scattering effect induced by structural motion will also be included. Thus, combining the forces into aeroelastic equation, the developed computational scheme can be tested on structure and for this study, the attention is toward typical wing models. In addition, this study is centered on computational results and no experimental outcomes will be involved. For the validation purpose, the generated results are compared with other existing data.

## **1.5 Thesis Hypothesis**

The thesis hypothesis is:

Flutter can be delayed to a higher velocity of the free stream under the influence of external acoustic source.

## **1.6 Thesis Outline**

This thesis is organized into five main chapters. In chapter 2, a comprehensive review is provided comprising literatures that are relevant to the understanding of this topic. The main objective of this chapter is to address the significant of this study and to explore the attempts done in the past for this particular matter. Furthermore, this chapter also discusses the theoretical background in the field of aerodynamics, acoustics and aeroelastic researches.

Chapter 3 demonstrated the computational methodology involved in this study. Three main sections are outlined to deal with three separated fields. The first section described the free vibration analysis while utilizing the FEM in creating the discrete structural model. Then, the second section explained the computational technique for aerodynamic analysis. The panel method is first described for steady flow and then extended for unsteady flow. For both cases, the two-dimensional and three-dimensional panel method will be presented. Afterward, the solution for aeroelastic problem while including the unsteady aerodynamic forces is presented using modal analysis. Meanwhile, the third section discussed the acoustical modeling using BEM. Here, the work is centered on the coupling procedure involving BEM, FEM and panel method formulations.

Subsequently, chapter 4 discussed the outcomes of the analyses performed using the formulations presented in the previous chapter. Here, the computational results for structural, aerodynamic and acoustic analyses were obtained. At the same time, the numerical investigation on aerodynamic performance by means of reduced frequency, airfoil profile and mean angle of attack are made to fulfill the secondary objectives of this study. Also, the applicability and reliability of panel method is evaluated as the results generated using MATLAB are then compared with existing data. Finally, the study concerned with the effect of acoustic on flutter analysis is demonstrated on selected wings and the results are discussed in detail.

Lastly, chapter 5 will draw a conclusion to this thesis and will discuss some possible extensions of the current work.

## Chapter 2

### LITERATURE REVIEW

#### 2.1 Unsteady Aerodynamics Prediction

To perform the aeroelastic analysis, one of the main considerations in modeling the aeroelasticity problem is associated with the prediction of aerodynamic loads. Since those early days when aeroelasticity phenomena arise, the unsteady aerodynamics and its interaction with elastic structure are then subjected to a great deal of interest. For the last half-century, a variety of approaches in formulating the unsteady aerodynamic forces have been proposed. Some of the early work on aeroelasticity was, in fact, based upon simple strip theory approximation. In two-dimensional strip theory aerodynamic, the lifting surface is modeled by a finite number of strips in the spanwise direction, and it is assumed that the unsteady aerodynamic forces on each strip are solely contributed by the motion of that strip. Together with other simplifying assumptions, the strip theory is often regarded as a very simple tool and easy to use. Thus, it is frequently employed for trend studies and basic understanding of aeroelastic instability. However, this theory is rather limited due to theoretical assumptions made and, therefore, it is only moderately accurate for low speed, high aspect ratio and unswept wings.

In the 1950s, Watkins, et al., (1959) formulated a numerical scheme based on kernel function of an integral equation using series expansions which is then known as the Kernel Function Method (KFM). According to their report, this kernel function is used to relate a known or prescribed downwash distribution to an unknown lift distribution for a harmonically oscillating finite wing of arbitrary geometry. Following the similar methodology, an improved numerical scheme was presented by Albano and

Rodden (1969) which is called Doublet Lattice Method (DLM), an extension of Vortex Lattice Method (VLM) where it is particularly designed for subsonic unsteady flow. Regarded as one of the most prominent approaches in predicting the unsteady airloads for aeroelastic analysis, the DLM is conveniently applicable on both planar and non-planar lifting surface. Based on this method, one may estimate the pressure distribution for a given vibration mode shape using the aerodynamic influence coefficients (AIC) calculated using a predefined model geometry. The calculation for pressure distribution can be repeated using the same AIC as it is purely aerodynamic related. Due to its simplicity, commercial software such as MSC/NASTRAN and ZAERO employed this particular method as the aerodynamic tool for subsonic aeroelastic analysis. Utilizing the computational code in commercial software, van Zyl (2008) extended the application of DLM in ZAERO to model complex configurations which includes the wind-body interference and the wake modeling. For further simplification, a much simpler method using similar approach as in the DLM known as Doublet Point Method (DPM) was formulated years later by Ueda and Dowell (1982). Although both use grids of boxes in trapezoidal shape to represent the surfaces, DPM offers a different approach by assuming the lifting pressure concentrated at a single point making the computational scheme more efficient but its accuracy reduced for the swept wing case. Hence, a hybrid method was proposed by Eversman and Pitt (1991) featuring the best combination of both method aiming to overcome the drawbacks in the traditional DLM and DPM.

Aside from using the acceleration potential of the flow, a different numerical scheme utilizing the velocity potential known as the velocity potential panel method was introduced in the article written by Jones and Moore (1973). For this particular method, a solving technique similar to DLM is used but would require an additional integration to

be carried out over the wake. In spite of that, the unsteady pressure distribution obtained from this computational scheme shows a better agreement with exact results if compared to those computed from KFM. Further implementation of similar approach can be seen in the work of Hounjet (1989) which focused on developing the computational code while refining the original method to accommodate a wider range of applicability in term of Mach number and frequency. For more compressive review on the development of unsteady airloads prediction, readers are directed to the work of Försching (1978). This author carried out an extensive study covering range of topics related to unsteady aerodynamics prediction including the applicability and reliability of various methods like KFM, DLM and velocity potential panel method. In more recent work, Cho and Williams (1993) developed a sophisticated approach in obtaining the unsteady influence coefficients and this is done by multiplying the steady influence coefficients with frequency-dependent phase factors. The scheme which can be implemented for subsonic and supersonic flow, is constructed especially for non-planar lifting surfaces and shows an excellent agreement with the previous schemes like doublet lattice, doublet point and a hybrid of the two. This particular technique is then employed to analyze the steady and unsteady aerodynamic analysis for different configuration of wings at subsonic, sonic and supersonic Mach numbers (Cho, et al., 2003). However, the field of unsteady aerodynamics for oscillating lifting systems and bodies still has plenty of limitations to deal with. One of the most significant drawbacks is the reliability of the resulted unsteady aerodynamic prediction.

In present aeroelastic simulation, the linear aerodynamics are commonly employed to predict unsteady aerodynamic loads for oscillating lifting system. However, the implemented techniques may not be adequate for future aeroelastic analysis with the

necessity of considering the strong nonlinearities of fluid flow at transonic regime and the importance of using the high fidelity equations. These have been addressed in the article written by Byun, et al. (1999) and they proposed an efficient procedure to compute the AIC using high fidelity equations (i.e. Euler or Navier-Stokes equations). With the swift progress of computer capability, it allows researchers to accurately model the additional features using higher-order methods. Unlike other approaches, this advanced technique presents an alternative computational method especially for analyzing more complex configurations in the transonic regime. Following so, Liu, et al. (2001) presented an effective method by integrating the computational fluid dynamics (CFD) and computational structural dynamics (CSD) simulation code for flutter calculation. The computational approach which based on a parallel, multiblock, multigrid flow solver for Euler/Navier-Stokes equations is capable of calculating conventional harmonic or indicial responses of an aeroelastic system, as well as performing direct CFD-CSD simulations. Furthermore, the CFD-based techniques now not only can be performed for static aeroelastic cases but also for the dynamic one (Livne, 2003). In another related work presented by Marques, et al. (2006), the CFD-based solution is implemented in aeroelastic analysis with main attention on frequency-domain analysis using the Fast Fourier Transform (FFT). Despite its supremacy, it requires more computational time. In fact, the unsteady high fidelity flow equations are extremely complicated from the theoretical and computational standpoint. For dynamic case, time-domain-based approach relies heavily on computation capability in which a complete cycle of computational effort is required for each time-step. For that reason, the CFD-based aeroelastic solution for three-dimensional case is computationally expensive. This challenge is addressed by Silva (2007) as significant improvements are



needed to reduce the computational cost. Therefore, it may not be the best option to consider the CFD-based techniques. In another attempt to produce an effective approach for aerodynamic pressure computation, Eller and Carlsson (2003) presented the aerodynamic solver for subsonic aeroelasticity application using boundary integral formulation. Like the CFD-based, the time-domain approach is preferred to overcome the nonlinear issue. However, this approach is still in the developing stage and may need some time to be fully constructed. Despite the limited capability, the tendency of using time-domain solution seen in CFD-based and BEM-based aeroelastic analysis can be regarded as the preference approach. It is well known that time-accurate calculations in three-dimensional problem is very time consuming and thus prevents CFD-based and new BEM-based approach from being used for this study. The implementation of these techniques in aeroelasticity analysis is only possible if the computational time and cost can be significantly reduced. To keep the computational time within realistic range, a simpler and reliable approach is needed to formulate the unsteady aerodynamic distribution while featuring in time domain.

Based on the discussion above, it is clear that there are a wide variety of numerical computation techniques for predicting of unsteady aerodynamic forces on oscillating lifting systems. Addressed by numerous researchers (Kuo and Morino, 1975; Försching, 1978; Eller and Carlsson, 2003), most of the numerical computational techniques are, however, tend to neglect the thickness effects of the lifting surfaces and they are often replaced by idealized plates of zero thickness. For a fairly thick structure, thickness of the lifting surface cannot be neglected anymore when taking the accuracy of aerodynamic modeling into consideration. Thus, most of the mentioned techniques are not ideally fit to be implemented for advanced aeroelasticity computational as we realize

that the profile thickness does affect both the steady-flow aerodynamic forces and the motion-induced unsteady aerodynamic forces. In general, the panel method is regarded as one of the most efficient and reliable technique in solving incompressible potential flow while assuming the viscous effects can be neglected and the flow is believed to be irrotational. Therefore, in the 1970s, Kuo and Morino (1975) pioneered the evolutionary step toward predicting the aerodynamic model with arbitrary configuration. In their report, the problem of a finite thickness wing in subsonic flow is analyzed for selected range of thickness ratio. Few years later, an approach using velocity potential panel method on three-dimensional harmonic oscillating thick wings for incompressible flow was documented in the article written by Giessler (1977). The implementation was a success where the three-dimensional velocity potential panel method produces a much better agreement with the experimental data compared with those from linearized lifting surface theory. A much detailed description of panel method can be obtained from textbook written by Katz and Plotkin (2001) in which they have done a comprehensive analysis of air flows past airfoils and wings using panel method. Furthermore, readers are also referred to the work of Cebeci and his associates (2005) which emphasize more on oscillating lifting surfaces for unsteady flow. To the best of our knowledge, no significant attempt has been done using panel method on three-dimensional wing geometry for aeroelastic study. Therefore, it served as an improvement from the previous technique and would provide a reliable approach in modeling the aerodynamic forces in this research work. In addition, this can be done with the advent of modern high-speed computers without dramatically increasing the computational cost.

## 2.2 Suppressing Flutter

As we discussed the vast selection of methods for unsteady aerodynamic prediction, it is worthwhile to look into the aeroelastic technology development in the aspect of flutter suppression before proceeding to the prospect of using acoustics in taming the aeroelastic threat. As mentioned earlier, heavier structure were purposely designed at the early age of airplane technology for flutter prevention. However, it doesn't complement with the desire to establish a highly-efficient and cost-effective flight. Therefore, various research efforts have been directed in designing the mechanisms for suppressing the flutter oscillations while enhancing fuel efficiency to achieve the desired flight performance. Thus, the idea of using active control system was put forward to replace the "passive" approach. Prior to designing the active control system, the profound understanding of aeroelastic modes that cause flutter is required and this depends greatly on representation of the unsteady aerodynamic loads which have been highlighted earlier. In earlier noteworthy work, the development is focused on constructing the aerodynamic transfer function representation from numerical data. In one of the most significant work documented, Karpel (1982) directed his concentration on the development of rational function approximations and utilize it for the purpose of aeroelastic control. Referring to his work, the state-space matrix equation of motion can be formed once a proper approximation for the aerodynamic loads is chosen. Using the state-space aeroelastic model, an active control system for simultaneous flutter suppression and gust alleviation can be designed by actively changing their characteristics in such a way that flutter occurs at a higher flight velocity. Making use of this minimum state formulation, it helps to minimize the computational time and cost.

Aside from this, many control mechanisms have been implemented to the problem of delaying flutter or controlling unstable wing motion. In another approach, Nissim (1971) introduced the aerodynamic energy concept to explain the active control systems by considering the energy aspect in the aeroelastic problem. According to his report, the aerodynamic energy approach can be used for investigating both the trailing-edge and leading-edge-trailing-edge control systems for flutter suppression and gust alleviation problems regardless of the different flight conditions considered.

In more recent study, the advance in the development and application of smart structures helps accelerate the prospect of active flutter suppression. One of the functional material called piezoelectric materials<sup>1</sup> have been tipped for having the potential to form actuation mechanisms for the purpose of flutter prevention due to their fast electromechanical response (Crawley and de Luis, 1987). Thus, Heeg (1993) further the investigation on the possibility of using piezoelectric plate actuators for this particular matter. In her report, a rigid wing model is attached with a flexible mount system which connected to spring tines (Fig. 2.1) to control the pitching degree of freedom and plunging motion in order to investigate flutter suppression using piezoelectric plates as actuators. The research which was conducted analytically and experimentally, proved to be a success as the flutter velocity could be increased by 20%. Then, Lazarus, et al. (1997) successfully suppressed vibration and flutter of the lifting surface with distributed strain actuators based on control methodology like Linear Quadratic Gaussian (LQG) technique. Likewise, Han, et al. (2006) investigated the implementation of piezoelectric actuation on a swept-back cantilevered lifting surface

---

<sup>1</sup> Piezoelectric materials are notably crystals and certain ceramics, which have the ability to generate electrical potential in response to applied mechanical stress.

following the study carried out by previous researchers. Meanwhile, in another attempt, Raja and Upadhyaya (2007) investigated the flutter suppression concept which integrates a stack mechanism actuated control surface as an aerodynamic effector. The results from wing-tunnel tests in a low speed subsonic flow regime shows that the concept can be implemented in any velocity regime or frequency band but there is room for improvement.

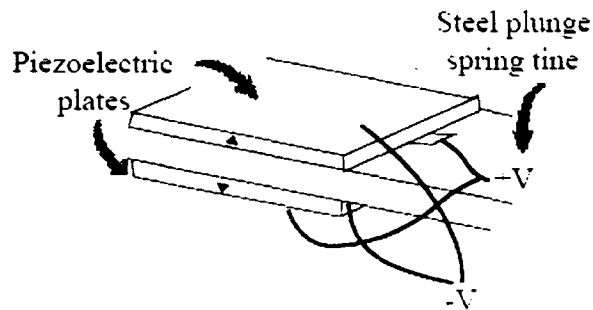


Figure 2.1: Schematic layout of piezoelectric actuator attachment. (Heeg, 1993)

Another interesting work reported on the flutter control mechanism using trailing edge flap is studied in the article written of Borglund and his colleague (2002). In their work, a simple aeroservoelastic analysis is carried out consisting controllable trailing edge flap which is attached to the cantilevered thin elastic wing with rectangular planform (illustrated in Fig. 2.2). Surprisingly, the proposed control strategy recorded significant result with an increase of an approximately 50% for the critical speed. However, further investigation is required as this major achievement was made possible by the fairly weak flutter instability. Aside from linear theory which has been successfully applied by most of the researchers in earlier discussion, study on active control system for nonlinear aeroelastic model was done by Block and Strganac (1998).

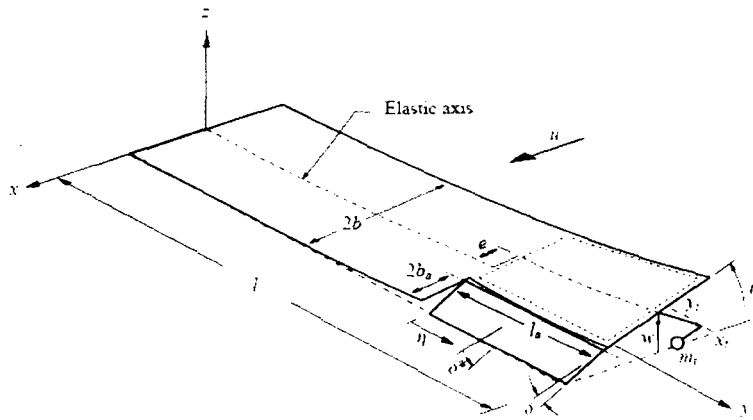


Figure 2.2: Schematic layout of cantilever wing with trailing edge flap. (Borglund and Kuttentkeuler, 2002)

From the discussion above, conventional active control techniques introduced which are driven by control law involving leading- and trailing-edge flaps, ailerons, spoilers, and others, are commonly used in modern aviation. However, the proposed control mechanisms are not without drawbacks. For instance, the piezoelectric material tends to be fragile under large tensile stress and the control surfaces driven by hydraulic power units are mostly sluggish and hence are not capable of handling the high-frequency oscillations (Lu and Huang, 1992). Furthermore, the control movements which aim to counteract the flutter motion would also cause changes in wing configuration which will also affect the total aerodynamic lift and moment variations (Stoia-Djeska, 2003). These leads in search for new concept of active flutter control. It is noted that to actively suppress the flutter motion, a quick response mechanism is required and it has been known for some time that the external acoustic excitation can in some cases be used to affect flutter (Livne, 2003). However, no solid study has been done in the past until Huang (1987) and his colleague (1992) presented the possibility of

using active acoustic excitations for flutter suppression. Before looking at the acoustics as the potential alternative flutter control technique, further discussions on acoustic effects on structure could help explore the true potential of this particular approach.

### **2.3 Acoustic Effects on Structure**

To exemplify the significance of this study, many of the earlier studies have been directed on acoustic excitation and its effects on structures. In simple words, acoustics can be described as the science concerned with the study of sound. Apparently, numerical methods such as FEM and BEM are typically used in solving the acoustical problem. However, they both present different approaches in this particular matter. The FEM is a differential-based numerical analysis technique which performs the numerical analysis first then followed by the integration of the governing differential equation. Unlike the FEM, the BEM is an integral-based of numerical analysis technique which involves a reverse procedure. For radiation problems, BEM is more preferable compared to FEM as the BEM is more efficient in handling the infinite domain problems (See the work of Yu, et al. (2010) for detailed description on this particular topic). Because of this matter, extensive researches and development works were carried out using BEM to construct the acoustics modeling techniques (Ali and Rajakumar, 2004). For acoustic problem, the BEM formulation based on the Helmholtz equation is frequently used. Generally, the simplest way used in solving the integral equation is by utilizing the conventional approach known as collocation BEM. Although the BEM formulation is mathematically complex, the solution is less time consuming. There exist numerous computational codes for acoustic BEM and one of them is demonstrated by Holmström (2001) using MATLAB. More recently, the development of a new BEM variant known

as fast multipole BEM by Fischer (2004) received lots of attention as this particular numerical technique is much quicker than the conventional BEM for large-scale problems and suitable for higher frequency applications. Other than that, the FEM which is suitable for bounded domains application is described in the work of Sandberg, et al. (2008).

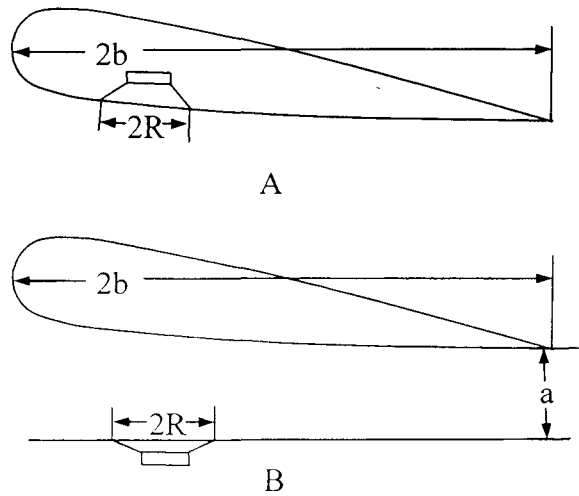


Figure 2.3: Loudspeaker mounted A) within the wing and B) in the wall of wind tunnel.  
(Huang, 1987)

For the past few decades, most of the preliminary investigations revealed that acoustic pressure produces significant influences on structures such as thin plate, membrane and also high-impedance medium like water (and other similar fluids). In this case, the system can be easily modeled using fully coupled technique where both FEM and BEM are frequently used. In general, the area of interest for this particular field is associated with the structural vibration which then leads to the introductory of acoustoelasticity study covering acoustic-structural interaction. Prominent studies in the field of acoustoelasticity can be found in the work written by Dowell, et al. (1977). They presented a general theoretical model in which structural-acoustic coupling system was



analyzed for interior sound fields. The applications of acoustoelasticity model can also be seen in various problems including sound propagation (Toupin and Bernstein, 1961), noise reduction (Lyon, 1963) and, as a potential instrument for measuring stress using ultrasonic wave (Man and Lu, 1987). However, for aerospace application, most of the studies carried out were due to the concern of the acoustic fatigue (Fahy and Wee, 1968; Rama Bhat, et al., 1973). To our best knowledge, the initial studies on structural analysis with the presence of acoustic excitation can be traced in the work of Fahy and Wee (1968) and also Rama Bhat, et al. (1973). Fahy and Wee (1968) investigated the responses of stiffened plates under intense acoustic excitation. The experimental works conducted by them concentrates in studying the effects of variations in stiffener configuration subjected to high frequency acoustic excitation. Meanwhile, Rama Bhat and his colleagues (1973) performed a theoretical investigation for the responses of structures like flat and stiffened plates in random acoustical environment. Afterward, the subsequent experimental study (Rama Bhat, et al., 1974) was done and the experimental data showed good agreement with theoretical results. Gradually, through these efforts, it was understood that the acoustics may have some significant effect on selective structures especially thin structures.

Following these early works, a newly advanced topic known as aeroacoustoelasticity that concentrates on aero-acoustic-structure interaction was established. This was demonstrated by Gennaretti and Iemma (2003) by taking additional consideration for the exterior aerodynamic flow using the CHIEF<sup>2</sup> regularization pioneered by Schenck (1968). Aside from theoretical contribution, Chou

---

<sup>2</sup> CHIEF (combined Helmholtz integral equation formulation) is a technique to filter out the spurious eigenvalues.

and his associates (2001) presented an experimental investigation on acoustic forcing of a thin aluminum plate by low-speed jets. The main objective of their study is to explore the connection between structural vibration of a thin aluminum plate in corresponding to the jet velocity and noise field in different orientations where it was tested at selected inclination angles. On the other hand, the previous works of Djojodihardjo (2007, 2008) demonstrated the acousto-aeroelastic problem using BE-FE approach had shown good preliminary results which could leads to significant influence on the performance of aeroelastic structure. However, relatively few publications have investigated the acoustic source as the potential prospect in handling the aeroelastic problem. Thus, continuing the previous work of Safari (2008), it is useful to investigate the acoustic effects on aeroelastic structure especially for the aircraft wing in a broader aspect.

## Chapter 3

### COMPUTATIONAL METHODOLOGY

#### 3.1 Analysis of free vibration

##### 3.1.1 Introduction

This section presents numerical modeling technique for aeroelastic structures. In general, aeroelastic structures, for example, the aircraft wing structures are often considered as plate-like structure. This is due to their thickness (or height) which is relatively small compared to the other spatial dimensions. In fact, the aircraft wing structures are not completely rigid and its elastic behavior is a major area of interest. Therefore, plate model is chosen for this study and it can be regarded as a three-dimensional body for the analysis purpose. Here, numerical approach is outlined using the finite element formulation for the plate structure modeling by utilizing four-node quadrilateral shell element. A detailed computational procedure is presented in preparation for the structural analysis where the analysis performed is mainly concentrated on vibration study concerning the natural frequencies and mode shapes. By doing so, this could assist in fulfilling the purpose of current work by first studying the dynamic characteristics of the structure model.

##### 3.1.2 Governing Equation of Motion

For a structural model, the governing equation of motion can be written, in general, as

$$\mathbf{M}\{\ddot{u}\} + \mathbf{C}\{\dot{u}\} + \mathbf{K}\{u\} = \{F\}, \quad (3.1)$$

where  $\mathbf{M}$ ,  $\mathbf{C}$ ,  $\mathbf{K}$  are mass, damping, and stiffness matrices while  $\{F\}$  is a vector of external forces. Also, the terms  $\{u\}$ ,  $\{\dot{u}\}$  and  $\{\ddot{u}\}$  denote the displacement, velocity and acceleration of the system. In this section, the attention is limited for the free vibration analysis as it is a vital preliminary study in order to investigate the vibrational characteristics of the plate before advancing toward forced vibration analysis afterward. Note that in free vibration, there are no external forces that act on the system and the damping coefficient can be neglected too. Thus, the equation of motion can be reduced and the simplified form can be presented as:

$$\mathbf{M}\{\ddot{u}\} + \mathbf{K}\{u\} = 0. \quad (3.2)$$

Having formulated the equation of motion for free vibration, it is now the task to define the mass and stiffness matrices using the isoparametric four-node quadrilateral shell element.

### 3.1.3 Isoparametric Four-Node Quadrilateral Shell Element

For FEM, in order to model the plate structure, the structure model is first discretized into finite elements where low order elements especially the standard four-node quadrilateral elements are frequently employed. Despite the rich variety of elements known, this particular element is chosen as it is one of the simplest element to generate and requires less computational effort compared to other elements. The flexibility of a general quadrilateral element can be illustrated in both the physical coordinates using the  $x-y$  coordinate axes shown in Fig. 3.1A and also in the undistorted space, using  $\xi-\eta$  axes in Fig. 3.1B.

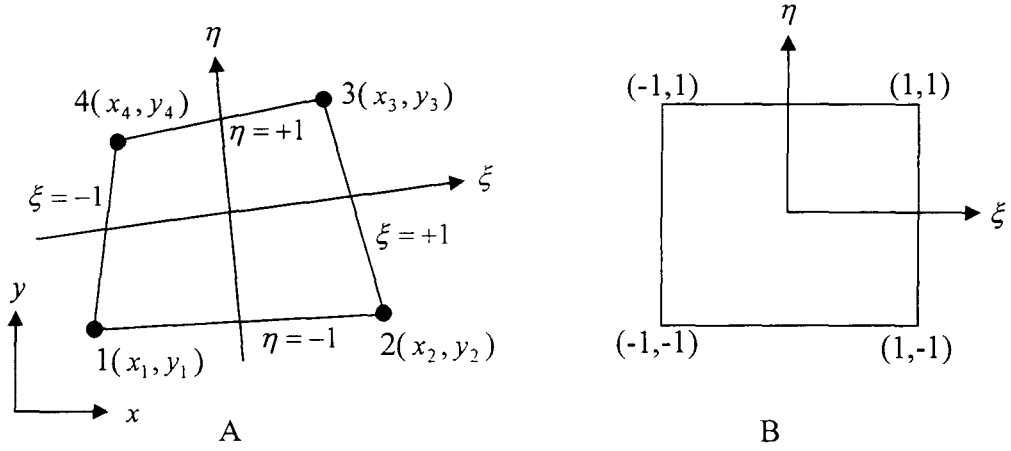


Figure 3.1: The four-node quadrilateral element: A) physical coordinates, B) isoparametric coordinates.

The Cartesian and the natural coordinates at each point are related in which the displacement shape functions are used to interpolate the element geometry in terms of the nodal coordinates. Thus, the nodal point within the four-node isoparametric quadrilateral element for both coordinate systems is given by

$$x = \sum_{i=1}^4 N_i(\xi, \eta) x_i, \quad y = \sum_{i=1}^4 N_i(\xi, \eta) y_i, \quad (3.3)$$

where  $(x_i, y_i)$  are the coordinates of node point  $i$  and  $N_i(\xi, \eta)$  are the standard displacement shape functions defined as

$$N_1 = \frac{1}{4}(1 - \xi)(1 - \eta); \quad (3.4a)$$

$$N_2 = \frac{1}{4}(1 + \xi)(1 - \eta); \quad (3.4b)$$

$$N_3 = \frac{1}{4}(1 + \xi)(1 + \eta); \quad (3.4c)$$

$$N_4 = \frac{1}{4}(1 - \xi)(1 + \eta). \quad (3.4d)$$

Applying the differential chain rule to the shape functions, one may write

$$\frac{\partial N_i}{\partial \xi} = \frac{\partial N_i}{\partial x} \frac{\partial x}{\partial \xi} + \frac{\partial N_i}{\partial y} \frac{\partial y}{\partial \xi}, \quad \frac{\partial N_i}{\partial \eta} = \frac{\partial N_i}{\partial x} \frac{\partial x}{\partial \eta} + \frac{\partial N_i}{\partial y} \frac{\partial y}{\partial \eta}, \quad (3.5)$$